The American Journal of Pathology, Vol. 173, No. 3, September 2008
Copyright © American Society for Investigative Pathology
DOI: 10.2353/ajpath.2008.080047

Immunopathology and Infectious Disease

Enhanced Nitrosative Stress during *Trypanosoma cruzi* Infection Causes Nitrotyrosine Modification of Host Proteins

Implications in Chagas' Disease

Monisha Dhiman,* Ernesto Satoshi Nakayasu,† Yashoda Hosakote Madaiah,‡ Brobey K. Reynolds,§ Jian-jun Wen,* Igor Correia Almeida,† and Nisha Jain Garg*§¶‖

From the Departments of Microbiology and Immunology, Pediatric Child Health Research,‡ Internal Medicine–Gastroenterology,§ Pathology,¶ and the Center for Biodefense and Emerging Infectious Diseases and the Sealy Center for Vaccine Development,‖ University of Texas Medical Branch, Galveston; and the Department of Biological Sciences,† The Border Biomedical Research Center, University of Texas at El Paso, El Paso, Texas*

Oxidative/nitrosative stress may be important in the pathology of Chagas' disease. Experimental animals infected by *Trypanosoma cruzi* showed an early rise in myocardial and peripheral protein-3-nitrotyrosine (3NT) and protein-carbonyl formation that persisted during the chronic stage of disease. In comparison, experimental chronic ethanol-induced cardiomyopathy was slow to develop and presented with a moderate increase in oxidative stress and minimal to no nitrosative stress after long-term alcohol feeding of animals. The oxidative stress in both chagasic animals and animals with ethanol-induced cardiomyopathy correlated with the persistence of reactive oxygen species-producing inflammatory intermediates. Protein-3NT formation in *T. cruzi*-infected animals was associated with enhanced nitric oxide expression (inferred by nitrite/nitrate levels) and myeloperoxidase activity, suggesting that both peroxynitrite- and myeloperoxidase-mediated pathways contribute to increased protein nitration in Chagas' disease. We used one- and two-dimensional gel electrophoresis and Western blot analysis to identify disease-specific plasma proteins that were 3NT-modified in *T. cruzi*-infected animals. Nitrated protein spots (56 in total) were sequenced by matrix-assisted laser desorption ionization/time of flight mass spectrometry and liquid chromatography–tandem mass spectrometry and identified by a homology search of public databases. Clustering of 3NT-modified proteins according to their functional characteristics revealed that the nitration of immunoglobulins, apolipoprotein isoforms, and other proteins might perturb their functions and be important in the pathology of Chagas' disease. We also showed that nitrated peptides derived from titin and α-actin were released into the plasma of patients with Chagas' disease. Such modified proteins may be useful biomarkers of Chagas' disease. ***(Am J Pathol 2008, 173:728–740; DOI: 10.2353/ajpath.2008.080047)***

Trypanosoma cruzi is the causative agent of Chagas' disease.[1] Infected hosts do not achieve a sterile immunity.[2] Factors implicated in the development of progressive chagasic cardiomyopathy include parasite persistence resulting in chronic inflammation of the heart, autoimmune response to self-antigens,[3] increased apoptosis and cell death,[4] and elevated levels of oxidative stress that may cause collateral damage to the heart.[5]

The host response to *T. cruzi* infection involves activation of macrophage and neutrophils. Reactive oxygen species (ROS) are elicited as a consequence of "respiratory burst" of activated phagocytic cells.[6,7] NADPH oxidase, produced by phagocytic macrophages, reduces O_2 to superoxide.[8] Myeloperoxidase (MPO), pro-

Supported by grant CON15420 from the John Sealy Memorial Endowment Fund (to N.J.G.) and in part by grant AI054578 from the National Institute of Allergy and Infectious Diseases (to N.J.G.) and grant 2SO6GM0812-37 from the National Institute of General Medical Sciences (to I.C.A.), National Institutes of Health (NIH). The Bimolecular Analysis Core Facility at the Border Biomedical Research Center, University of Texas at El Paso, is supported by grant 5G12RR008124 from the National Center for Research Resources, National Institutes of Health.

Accepted for publication June 11, 2008.

Address reprint requests to Dr. Nisha Jain Garg, 3.142C Medical Research Building, University of Texas Medical Branch, 301 University Boulevard, Galveston TX 77555-1070, E-mail: nigarg@utmb.edu.

duced by activated neutrophils, uses H_2O_2 and chloride (Cl^-) ions, and the major end product is the highly reactive hypochlorous acid (HOCl).[9] Superoxide and HOCl can also react to form a hydroxyl radical.[10] These cytotoxic ROS and nitric oxide (NO) synthesis by inducible nitric oxide synthase (iNOS) during inflammatory responses are proposed to contribute to control of *T. cruzi* infection,[11] although some studies have indicated that parasites express peroxyredoxins to prevent the ROS-mediated injurious process.[12]

The ROS and reactive nitrogen species (RNS) may have direct toxicity for the host cellular components.[13] Multiple defense mechanisms to control oxidative injurious processes are present in the host cells, yet excessive ROS/RNS production or compromised antioxidant system would result in inefficient removal of free radicals and oxidative/nitrosative damage. In human patients with Chagas' disease, antioxidant/oxidant imbalance is evidenced by increased plasma levels of glutathione disulfide and malonyldialdehyde[14] and decreased levels of glutathione[14,15] and glutathione peroxidase.[15,16] In studies involving experimental models of Chagas' disease, increased levels of phospholipid oxidation products and protein carbonylation products in heart tissue[17] were shown to be associated with oxidative overload[18] and inefficient glutathione antioxidant defense.[17] Treatment with antioxidants (phenylbutylnitrone, vitamin C, and vitamin E) attenuated the oxidative effects in both experimental models[18] and human patients with Chagas' disease.[19] Others have shown the macrophage activation of ROS/RNS and peroxynitrite ($ONOO^-$) formation during *T. cruzi* infection[20] was associated with increased protein 3-nitrotyrosine (3NT) levels in the heart of infected mice.[21] Accordingly, defining targets of oxidative/nitrosative modification in Chagas' disease and the potential functional consequences that may result is of considerable interest.

In this study, we aimed to identify the protein targets that are modified during progressive Chagas' disease. Our data show that the induction of inflammatory mediators is associated with a substantial increase in protein-3NT and protein-carbonyl formation in chagasic heart and plasma. The extent of nitrosative stress in chagasic animals was significantly higher than that observed in animals with other cardiomyopathies. By two-dimensional gel electrophoresis (2D-GE)/Western blotting and mass spectrometric [matrix-assisted laser desorption ionization/time of flight (MALDI-TOF mass spectrometry) and liquid chromatography–tandem mass spectrometry (LC-MS/MS)] approaches, we have identified plasma proteins that are 3NT-modified in a disease-specific manner, and these would likely be useful biomarkers of the acute and chronic Chagas' disease state. We discuss the pathological significance of protein nitration in Chagas' disease.

Materials and Methods

Animals and Parasites

Six- to-8-week old C3H/HeN mice or Sprague-Dawley rats (Harlan Laboratories) were infected with culture-derived *T. cruzi* trypomastigotes (SylvioX 10/4 strain, 10,000 parasites/animal, intraperitoneally). Animals were sacrificed during acute infection [mice, 27–35 days postinfection (dpi); rats, 45 dpi] or chronic disease (6 months postinfection) phase. For some studies, Sprague-Dawley rats were provided alcohol in drinking water (12%, v/v) for 24 months,[22] and tissues harvested. Animal experiments were performed according to the National Institutes of Health Guide for Care and Use of Experimental Animals and approved by the University of Texas Medical Branch Animal Care and Use Committee.

Plasma Collection and Albumin Depletion

Blood samples were collected in the presence of K_3EDTA and protease inhibitor cocktail (Sigma Chemical Co., St. Louis, MO P-2714), centrifuged at 2500 $\times$ *g* for 15 minutes at 4°C, and supernatant harvested. Plasma samples were incubated sequentially for 1 hour each at 4°C with 0.1 mol/L NaCl and 42% ethanol and centrifuged at 16,000 $\times$ *g* for 45 minutes at 4°C. Supernatants were transferred to new tubes, acidified to pH 5.7 using 0.8 mol/L CH_3COONa (pH 4.0), incubated for 1 hour at 4°C, and centrifuged as above. Albumin-containing supernatant fraction was transferred to new microtubes. The pellets from first and second centrifugation steps were combined and resuspended in 10 mmol/L Tris buffer, pH 6.8, and 1 mol/L urea.[23] All samples were stored at −70°C until further use. Protein content was determined using the Bradford assay (BioRad Hercules, CA).

Immunohistochemistry and Histopathology

Cryostat tissue sections (5 μm) were treated with 0.3% H_2O_2/phosphate-buffered saline and avidin/biotin (Vector Laboratories Burlingame, CA) to block the endogenous reactions and incubated with rabbit anti-3NT antibody (1:1000, Millipore Billeria, MA) for 12 hours. After washing with distilled water, sections were incubated for 30 minutes each at room temperature with biotinylated anti-rabbit IgG and horseradish peroxidase-conjugated streptavidin (1:150, DAKO Carpinteri, CA). Slides were rinsed with phosphate-buffered saline and distilled H_2O, and color was developed using diaminobenzidine substrate. Tissue sections were counterstained with hematoxylin.

Enzyme-Linked Immunosorbent Assay (ELISA)

Plasma samples were treated with dinitrophenyl hydrazine (DNPH) to derivatize the carbonyl proteins. Dinitrophenyl-derivatized carbonyl proteins and 3NT-modified proteins were detected by ELISA. Briefly, plasma samples were added in triplicate (100 μl/well). Plates were blocked with 1% gelatin or reduced bovine serum albumin, and incubated with polyclonal anti-DNP antibody (Sigma Chemical Co.; 1:1000) or anti-3NT antibody (1:4000 dilution, Millipore).[21,24] After incubation with horseradish peroxidase-conjugated secondary antibody, color was developed with Sure Blue TMB substrate (Kirkegaard & Perry Gaithersburg, MA) and absorbance recorded at 650 nm using a SpectraMax 190 microplate

reader (Molecular Devices Sunny Dale, CA). Bovine serum albumin (Sigma Chemical Co.; fatty acid–free) derivatized with 50 mmol/L $NaNO_2$, 10 mmol/L H_2O_2, and 100 μmol/L horseradish peroxidase was used as a positive control.[25]

Enzymatic Assays

All enzymatic assays were conducted in 96-well microtiter plates using plasma samples in triplicate (10 μg of protein/well). Nitrite/nitrate level, indicative of NO production by iNOS enzyme, was monitored by the Griess reagent assay.[26] Briefly, plasma samples were incubated with spongy cadmium to reduce nitrate to nitrite[27] and incubated with 100 μl of Griess reagent (1% sulfanilamide in 5% phosphoric acid and 0.1% *N*-1-napthyl ethylenediamine dihydrochloride, 1:1,v/v). The change in absorbance was monitored at 545 nm (standard curve, 0–200 μmol/L sodium nitrite). To measure MPO activity, plasma samples ([10 μg of protein) were incubated with 0.53 mmol/L *O*-dianisidine dihydrochloride (Sigma)/0.15 mmol/L H_2O_2 in 50 mmol/L potassium phosphate buffer (pH 6.0). Reaction was stopped with 30% sodium azide, and the change in absorbance measured at 460 nm (ε = 11,300 $M^{-1} \cdot cm^{-1}$).[28] To measure xanthine oxidase (XOD) activity, plasma samples were incubated with 0.15 mmol/L xanthine in 50 mmol/L phosphate buffer (pH 7.5), and the rate of uric acid production was recorded at 290 nm (ε = 12,200 $M^{-1} \cdot cm^{-1}$).[29]

One- and 2D-GE and Western Blotting

Tissue homogenates or plasma samples (5 μg of protein) were resolved on 10% acrylamide gels on a mini-Protean 3 system (BioRad) using 0.2 mol/L Tris-HCl anode buffer (pH 8.8) and 0.1 mol/L Tris-Tricine cathode buffer containing 0.1% sodium dodecyl sulfate. Gels were stained with 0.005% Coomassie blue G250 (BioRad) and images were acquired using a FluorChem 8800 image analyzing system (Alpha Innotech).

The 7-cm (pH 3–10) immobilized pH gradient strips (BioRad) were rehydrated at 50 V for 12 hours with 250 μl of lysis/rehydration buffer (2 mol/L thiourea, 7 mol/L urea, 4% 3-[(3-cholamidopropyl)dimethylammonio]propanesulfonate, 0.5% Triton X-100, 1% dithiothreitol, and 0.5% ampholytes; BioRad) containing a 100 μg of protein sample and a trace amount of bromophenol blue. Isoelectric focusing was performed on the strips as follows: 500 V for 1 hour, 1000 V for 1 hour, 8000 V for 2 hours, and then at 8000 V for a total of 50,000 Vh. After isoelectric focusing, immobilized pH gradient strips were sequentially coated with sodium dodecyl sulfate for 15 minutes each in equilibration buffer (50 mmol/L Tris-HCl, pH 8.8; 6 mol/L urea; 30% glycerol; 2% sodium dodecyl sulfate) containing 1% dithiothreitol (reducing conditions) and 2% iodoacetamide (alkylating conditions). Equilibrated strips were subjected to second-dimension electrophoresis using 8 to 10% linear gradient precast Tricine gels (BioRad) on a Criterion cell system at 75 V for 1 hour and then at 120 V until the dye front reached the bottom of the gel. Gels were fixed in 10% methanol/7% acetic acid, stained with SYPRO Ruby (BioRad), destained in 10% ethanol, and imaged using a high-resolution ProXPRESS proteomic imaging system (Perkin Elmer). The comparative analysis of different gel images was performed using Progenesis Samespots software (Nonlinear Dynamics). The resultant data were further managed and analyzed using the GenoLogics Proteus proteomics solution.

Samples resolved by 1D-GE or 2D-GE were transferred to polyvinylidene difluoride membranes using a wet vertical Criterion Blotter (BioRad). Membranes were blocked for 1 hour with 5% nonfat dry milk (BioRad) in 50 mmol/L Tris-HCl (pH 7.4) containing 150 mmol/L NaCl and 0.05% Tween 20 (TBST). All antibody dilutions were made in 5% nonfat dry milk-TBST. Membranes were incubated (4°C overnight) with the following primary antibodies: mouse anti-3NT monoclonal antibody (1:5000, clone 1A6), rat anti-3NT antibody (1:5000, Millipore), and mouse anti-ApoAI antibody (1:5000, Biodesign International Saco, Maine). The DNP-derivatized carbonyl proteins were probed with rabbit anti-DNP antibody (1:4000, Sigma).[17] Membranes were washed with TBST, incubated with horseradish peroxidase-conjugated secondary antibody (1:15,000, Southern Biotech Birmingham, AL) for 1 hour, and signal was developed by an enhanced chemiluminescence detection system (GE Healthcare, Piscataway, NJ).

Mass Spectrometry

Gel spots (≤1 mm) were incubated at 37°C for 30 minutes each in 100 μl of 50 mmol/L NH_4HCO_3, followed by 100 μl of dH_2O. Gel spots were then dehydrated in 100 μl of acetonitrile twice for 5 minutes each, dried, and in-gel proteins were digested with 100 ng of trypsin in 25 mmol/L NH_4HCO_3 at 37°C for 6 hours. Peptides were analyzed by either a MALDI-TOF-MS tandem mass spectrometer (ABI 4800 Proteomics Analyzer, Applied Biosystems Foster City) or by nanoLC-MS/MS using an LTQ (Thermo Fisher) or an LTQXL (Thermo Fisher Pittsburgh, PA) electrospray ionization-linear ion trap mass spectrometer. For MALDI-TOF-MS, peptide samples were purified with a ZipTip (Millipore) and reconstituted with 0.4% acetic acid before analysis. A 1:1 dilution of peptide solution with MALDI matrix solution (Agilent Technologies Santa Clara, CA) was used for MALDI spotting and analyzed at the Protein Chemistry Laboratory of the Biomolecular Resource Facility, University of Texas Medical Branch.

For LTQ analysis, an in-house fabricated nanoelectrospray source and an HP1100 solvent delivery system (Agilent Technologies) were coupled to LTQ. Samples were automatically delivered by a FAMOS autosampler (LC Packings, Dionex) to a 100-μm internal diameter fused silica capillary precolumn packed with 2 cm of 200-Å pore size Magic C18AQ material (Michrom Bioresources Auburn, CA). The samples were washed with solvent A (5% acetonitrile in 0.1% formic acid) on the precolumn, eluted with a gradient of 10 to 35% solvent B (100% acetonitrile) over 30 minutes to a 75-μm × 10-cm fused silica capillary column packed with 100-Å pore size Magic C18AQ material (Michrom Biore-

sources), and then injected into the mass spectrometer at a constant column tip flow rate of ~300 nl/min. Eluting peptides were analyzed by nanoLC-MS and data-dependent nanoLC-MS/MS acquisition, selecting the three most abundant precursor ions for MS/MS with a dynamic exclusion setting of 1 minute.[30]

For LTQXL analysis, peptide samples were loaded into a C18 trap column (1 μl C18, OPTI-PAK) and washed for 10 minutes with 2% acetonitrile/0.1% formic acid at 5 μl/min. The separation was performed in a capillary reverse-phase column (Acclaim, 3 μm C18, 75 μm × 25 cm, LC Packings, Dionex Sunny Vale, CA) connected to a nanoLC system (nanoLC 1D plus, Eksigent Technologies Dublin, CA). Peptides were eluted in a gradient solvent of 0 to 40% (solvent A, 2% acetonitrile/0.1% formic acid; solvent B, 80% acetonitrile/0.1% formic acid) for 30 minutes and directly analyzed in the LTQXL. MS spectra were collected in centroid mode in a range from 400 to 1700 *m/z*, and the three most abundant ions were submitted twice to fragmentation (35% normalized collision energy) before dynamically excluded for 120 seconds.

The peptide mass profiling data were submitted to Mascot (Matrix Science) and searched against NCBI database using GPS Explorer (version 3.6, Applied Biosystems). The criteria for positive identification of the proteins was a MOWSE score of >42, as calculated by a Mascot scoring algorithm, mass accuracy of 50 ppm, and mapping of at least two peptides/protein. All identified protein sequences were compared using a BLAST tool[31] at the NCBI database. Sequences with low BLAST scores were re-analyzed at GeneDB. All MS/MS spectra from peptides with 600 to 3500 da and at least 15 fragments were converted into DTA files using Bioworks version 3.3.1 (Thermo Fisher). The DTA files were submitted to database search using TurboSequest[32] (available in Bioworks) against the mouse IPI version 3.25 (*http://www.ebi.ac.uk/IPI/IPImouse.html* Jan 2007) and TcruziDB version 5.0 (*http://tcruzidb.org* Aug 2005) databases, concatenated with the reverse version of the same databases. The parameters for database search were: one missed cleavage site for trypsin digestion, carbamidomethylation of cysteine residues as fixed modification, and oxidation of methionine and nitrosylation of tyrosine residues as variable modifications. Mass tolerance was set to 2.0 and 1.0 da for intact peptides and fragment ions, respectively. The following filters were applied in Bioworks for protein validation: $DC_n \geq 0.1$; protein probability $\leq 1 \times 10^{-3}$; and $X_{corr} \geq 1.5$, 2.0, and 2.5 for singly-, doubly- and triply-charged peptides, respectively. With these parameters, no false positive hits were observed.

Statistical Analysis

Five to eight animals were included in each experimental group. All experiments were repeated at least three times. Data are presented as mean values ± SD. The results were compared by Mann-Whitney-Wilcoxon test, and $P \leq 0.05$ was considered significant.

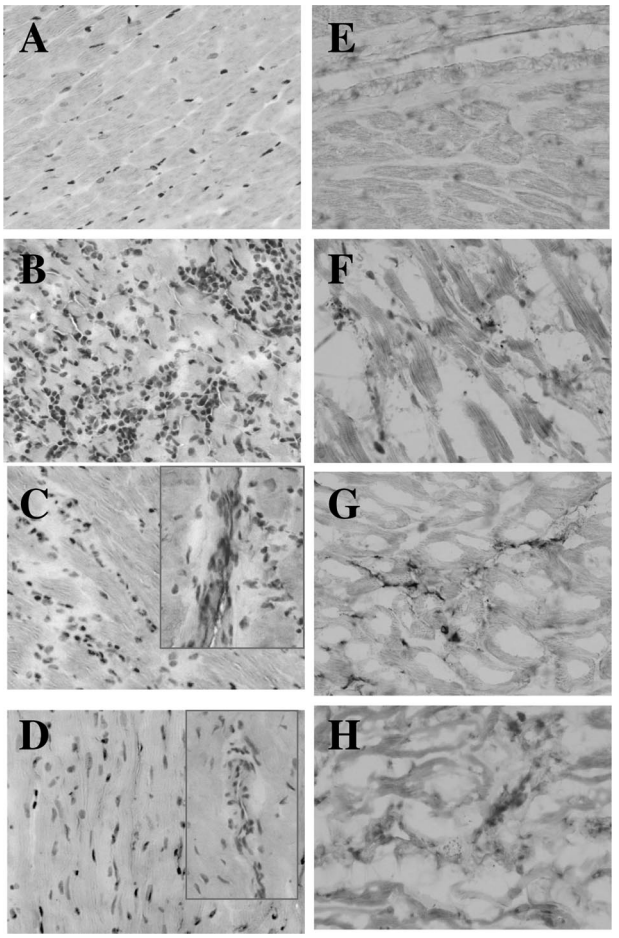

Figure 1. Histological analysis. Sprague-Dawley rat were infected with *T. cruzi* or fed ethanol in drinking water. Cryostat sections of the heart tissue were subjected to hematoxylin and eosin staining (**A–D**) and immunohistological staining with anti-nitrotyrosine antibody (**E–H**). Shown are micrographs from normal rats (**A** and **E**), rats with acute (45 dpi, **B** and **F**) and chronic (150 dpi, **C** and **G**) *T. cruzi* infection, and rats with chronic alcohol feeding for 24 months (**D** and **H**). **C** and **D** show the infiltration of inflammatory infiltrate in chronic heart. Original magnification, ×10.

Results

Histopathological analysis of cardiac tissue sections from *T. cruzi*-infected and ethanol-fed animals is shown in Figure 1, A–D. The acutely infected animals (45 dpi) exhibited an extensive infiltration of inflammatory infiltrate in the myocardium (Figure 1B). Some of the inflammatory foci were associated with parasitic nests. During chronic stage (6 months pi), chagasic animals maintained a moderate level of diffused inflammatory response associated with tissue fibrosis and cell death (Figure 1C). The effect of ethanol was evident after long-term feeding for 24 months when animals exhibited a modest tissue fibrosis and scattered inflammation in the heart (Figure 1D).

As a first step in investigating the oxidative/nitrosative stress, we monitored the cardiac level of protein modifications in chagasic animals. In agreement with inflammatory responses, a very high level of protein nitration was detected in the myocardium of acutely infected animals (Figure 1F). In chronic chagasic myocardium, though lesser than that detected in acute phase, the extent of

protein nitration was significantly higher than the normal controls (compare Figure 1, G and E, respectively). Ethanol-fed rats exhibited minimal to no nitration of cardiac proteins (Figure 1H). Comparison of the immunoreactivity for DNP-derivatized carbonyl proteins using anti-DNP antibody showed a significant increase in the protein oxidation level in chagasic and ethanol-induced cardiomyopathy (EICM) hearts as compared to controls. The extent of protein carbonylation in chronically infected and ethanol-fed animals was not disease-specific (data not shown). Together, these results suggest that *T. cruzi* infection elicits strong inflammatory responses and oxidative/nitrosative stress that persist in the heart during chronic phase. Alcohol-induced cardiomyopathy is slow in development and is associated with mild inflammatory and oxidative responses and minimal nitrosative stress.

In agreement with the cardiac results, plasma level of protein nitration was increased in *T. cruzi*-infected animals. The 3NT-modified proteins, determined by ELISA, were increased by 272% and 142% in plasma of acutely and chronically infected chagasic animals, respectively. Protein-3NT level in EICM plasma was not significantly different as compared to controls (Figure 2A). Western blot (WB) analysis with anti-3NT antibody validated the ELISA results. By WB, we detected approximately threefold increase in nitration of several proteins in chagasic plasma as compared to that detected in normal controls (Figure 2B, arrows). In plasma of chronic ethanol-fed animals, the pattern of 3NT-modified proteins was similar to that noted in normal controls (Figure 2B). Specificity of the anti-3NT antibody was validated by a loss in signal on pretreatment of the nitrated bovine serum albumin with 20 mmol/L dithionite that reduces 3-nitrotyrosine to 3-aminotyrosine, not detectable by anti-3NT antibody, also described in a previous study.[33] Coomassie blue staining of

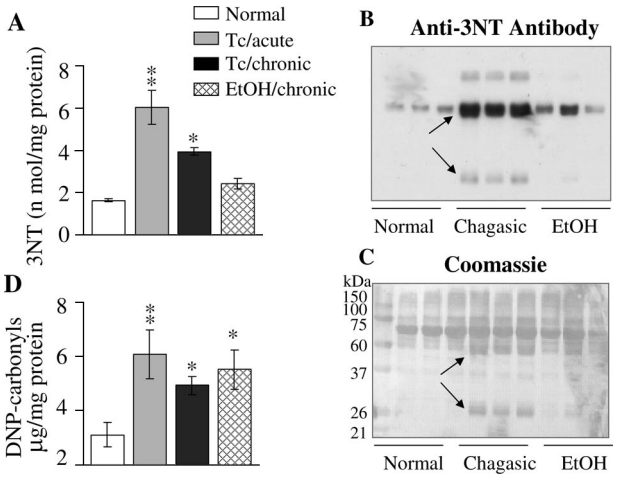

Figure 2. Plasma protein nitration is increased in chagasic rats. **A:** ELISA was performed for 3NT-protein detection in plasma samples from *T. cruzi*-infected acute and chronic rats and rats chronically fed with ethanol (EtOH). **B:** Plasma samples were resolved by 10% sodium dodecyl sulfate-polyacrylamide gel electrophoresis, and Western blot analysis was performed with anti-nitrotyrosine antibody. Coomassie blue staining of the membrane is shown in **C**. **Arrows** indicate the differentially expressed/modified proteins in chagasic plasma. **D:** Plasma samples were treated with dinitrophenyl hydrazine, and DNP-derivatized carbonyl-proteins detected by an ELISA using an anti-DNP antibody. Data (mean ± SD) are representative of three independent experiments. $^{*}P < 0.05$; $^{**}P < 0.01$.

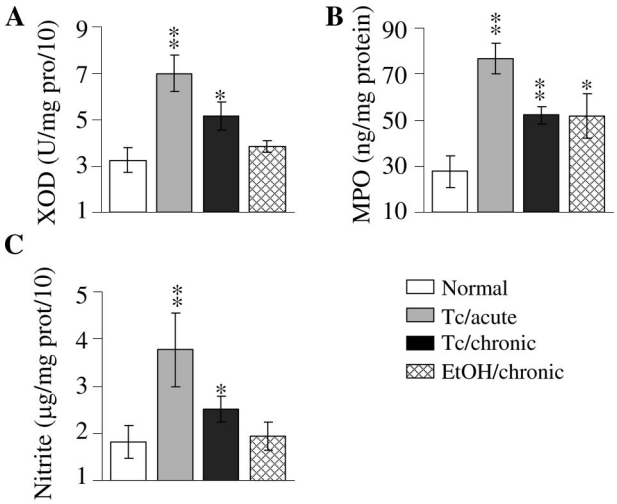

Figure 3. Inflammatory mediators in chagasic plasma. Plasma samples were obtained from normal rats, *T. cruzi*-infected rats during acute (45 dpi) and chronic (150 dpi) stages, and the ethanol-fed chronic (24 months after treatment) rats. The specific activities of XOD (**A**) and MPO (**B**) enzymes and the nitrite level (**C**) were determined as described in Materials and Methods. Data (mean ± SD) are representative of three independent experiments. $P < 0.05$; $^{**}P < 0.01$.

the membranes verified equal loading of all protein samples and showed that some of the 3NT-modified proteins were uniquely expressed in chagasic samples (Figure 2C, arrows). Comparison of the immunoreactivity for carbonyl proteins by ELISA (Figure 2D) and Western blotting (data not shown) showed a similar extent and pattern of protein oxidation in chagasic and EICM plasma. These results validate that protein oxidation occurs in *T. cruzi*-induced Chagas' disease and EICM and that nitrosative stress is induced in a disease-specific manner.

We measured the activities of the XOD, MPO (source of oxidants), and nitrate/nitrite level (indicative of iNOS-mediated NO production) to identify the intermediates involved in the formation of ROS/RNS in chagasic and EICM conditions. The increase in protein-3NT formation in acute chagasic plasma was paralleled by 116%, 178%, and 101% increase in XOD, MPO, and iNOS (inferred by nitrite level) activities, respectively (Figure 3). In chronic chagasic plasma, we noted 59% and 88% increase in XOD and MPO activities that was comparable to that detected in EICM plasma samples (Figure 3, A and B). Noticeably, nitrite level was significantly increased in chronic chagasic plasma (47% increase), but not in the EICM samples, when compared to those detected in normal control plasma (Figure 3C). These results suggest that ROS-producing intermediates (XOD, MPO) are increased in both *T. cruzi*-infected and ethanol-fed animals, while RNS-producing intermediate (ie, iNOS) is mainly enhanced in Chagas' disease of infectious etiology.

Toward identifying the plasma proteins that are nitrosylated and may be diagnostic of disease state and/or pathology, we proceeded to develop the plasma proteome. The plasma dynamic range of proteins over 10 orders of magnitude makes it difficult to achieve an in-depth proteomic analysis. To facilitate the resolution and identification of low-abundance proteins, we used a chemical-based extraction method for the removal of

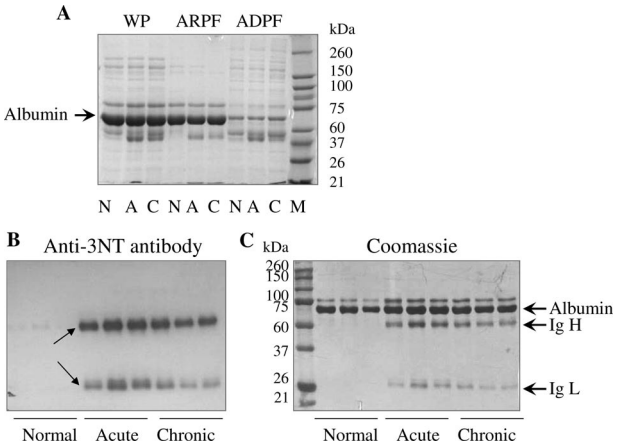

Figure 4. A: Fractionation of plasma and enrichment of low to abundant proteins. C3H/HeN mice were infected with *T. cruzi* and sacrificed during the acute **(A)** or chronic **(C)** stages. Plasma samples were collected on K_3EDTA, and the abundant proteins removed as described in Materials and Methods. WP, whole plasma; ARPF, albumin-rich plasma fraction; ADPF, albumin-depleted plasma fraction; N, normal mice. **B** and **C:** Nitration of albumin-rich plasma fraction from chagasic mice. The albumin-rich plasma fractions from normal and infected (acute and chronic) mice were resolved by sodium dodecyl sulfate-polyacrylamide gel electrophoresis, and Western blot analysis was performed using mouse anti-3-nitrotyrosine antibody (**B**). Coomassie blue stain of the membranes is shown in **C**. **Arrows** indicate the protein bands that were submitted to mass spectrometry. Data are representative of three independent experiments.

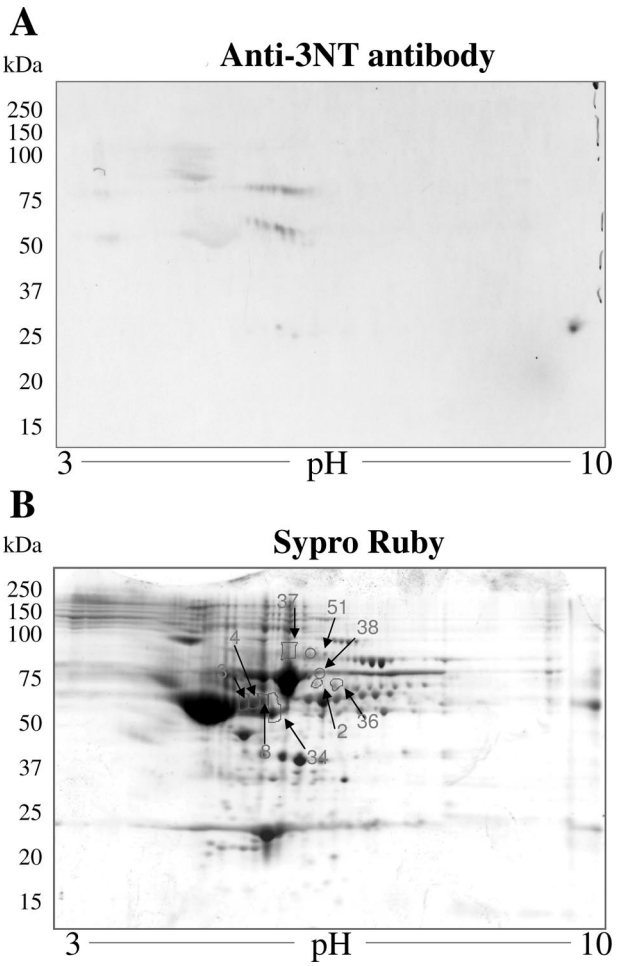

Figure 5. Plasma proteome from normal mice. Dealbuminated plasma samples from normal mice were resolved by 2D-GE, and proteins were transferred to polyvinylidene difluoride membrane. Shown are the representative images from Western blot analysis with anti-nitrotyrosine antibody **(A)** and gel-staining with SYPRO Ruby **(B)**. Plasma proteins that were nitrated (marked with **arrow** and numbered in **B**) were identified by mass spectrometry (Tables 1 and 2). Data are representative of three independent experiments.

albumin, the most abundant protein in the serum. As shown in Figure 4A, the albumin-rich plasma fraction consisted of >90% albumin, resulting in a better resolution of less abundant proteins in the albumin-depleted plasma fraction. The comparative pattern of nitration versus protein concentration for albumin-rich plasma fractions from chagasic samples is shown in Figure 4, B and C. The 66-kd albumin was present at equal concentration in all samples (Figure 4C) and appeared to be not heavily nitrated in chagasic plasma (Figure 4B). Of the three additional bands in chagasic albumin-rich plasma fraction, two bands (55 and 21 kd) were found to be differentially expressed as well as nitrated when compared to normal albumin-rich plasma fraction. Protein sequencing identified 55- and 21-kd bands as heavy and light immunoglobulin chains, respectively.

The complex mixture of proteins in albumin-depleted plasma fractions from normal and chagasic animals were not appropriately resolved by 1D-GE (data not shown), and thus we performed 2D-GE. Representative 2D-gel images of WB analysis using anti-3NT antibody (A) and SYPRO Ruby staining (B) of plasma from normal mice (Figure 5), and acutely (Figure 6) and chronically (Figure 7) infected animals are shown. The gel images were superimposed according to relative molecular mass and isoelectric point (pI), and a grid corresponding to the exact dimension of the gels was used to overlay the images. Comparative densitometric analysis of SYPRO Ruby staining versus immunoreactivity with anti-3NT antibody identified protein spots that were differentially expressed/nitrated in a disease state-specific manner (Tables 1 and 2). In general, the extent of nitration of various proteins was more pronounced in acute plasma and continued to persist during chronic stage of disease development (Tables 1 and 2). These protein spots were excised from the SYPRO Ruby-stained gels, were digested in gel with trypsin, and tryptic peptides were analyzed by mass spectrometry. Of the 56 proteins submitted to mass spectrometry, 39 were identified by MALDI-MS/MS (Table 1). An additional 11 proteins were identified by LC-MS/MS analysis (Table 2). Six of the 56 (spot 51–56) protein spots were not identified by either of the mass spectrometric approaches.

Our data show that immunoglobulin (antibody) family members, including IgG and IgA light chains, IgG-γ, -γ2a, and -γ3 heavy chains, and IgH-6 (spots 9–22), were nitrated in chagasic plasma. Comparative densitometric analysis of the images from WB with anti-3NT antibody (panel A in Figures 5–7) showed that the nitration of several immunoglobulin light and heavy chains was two- to sixfold higher in infected mice as compared to the normal controls. The extent of nitration of the immunoglobulins was significantly higher in acute mice than in the chronic mice (Table 1). We noted increased

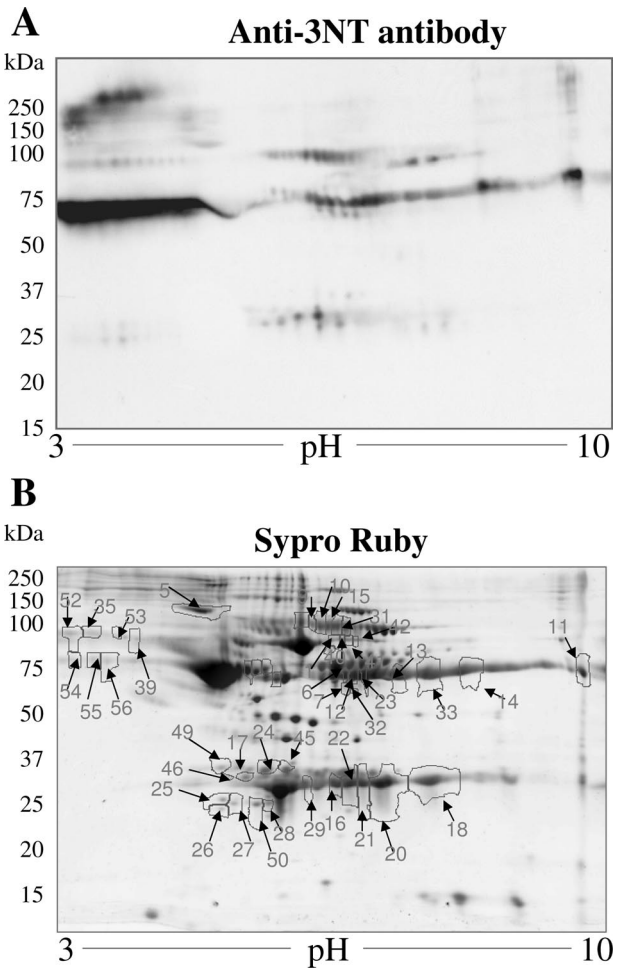

Figure 6. Plasma proteome from *T. cruzi*-infected acute mice. Dealbuminated plasma samples from acutely infected mice (25–30 dpi) were resolved by 2D-GE. Shown are the representative images from WB analysis with anti-3NT antibody **(A)** and gel staining with SYPRO Ruby **(B)**. Nitrated proteins (marked with **arrow** and numbered in **B**) were identified by mass spectrometry (Tables 1 and 2). Data are representative of three independent experiments.

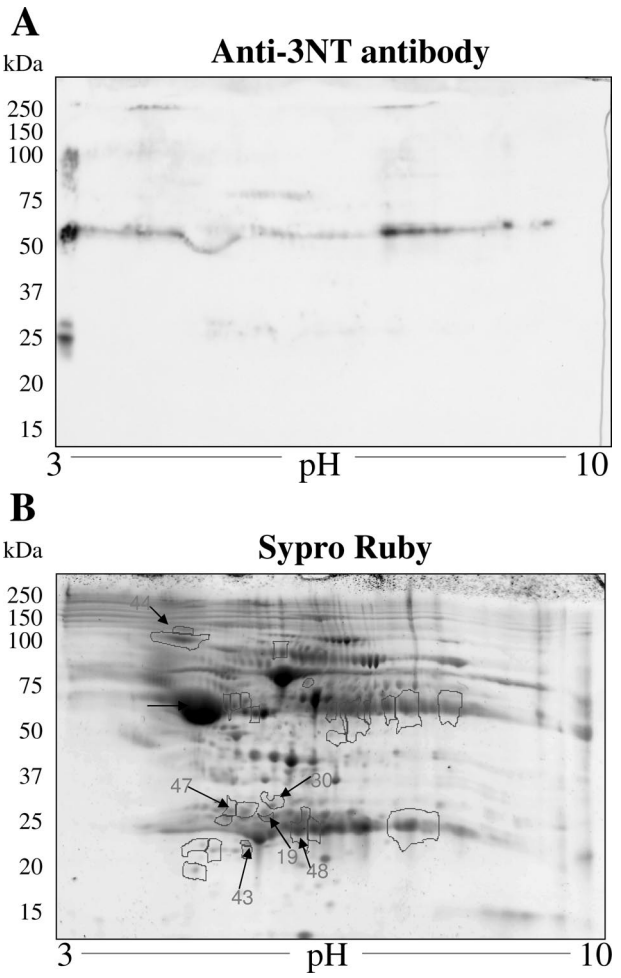

Figure 7. Plasma proteome from *T. cruzi*-infected chronic mice. Dealbuminated plasma samples from chronically infected mice (150 dpi) were resolved by 2D-GE. Shown are the representative images from WB analysis with anti-3NT antibody **(A)** and gel staining with SYPRO Ruby **(B)**. Nitrated proteins (numbered) were identified by mass spectrometry (Tables 1 and 2). Data are representative of three independent experiments.

nitration of C3b (spot 23), which is a member of both classical and alternate complement pathways. Two proteins, identified as Igκ light chain (spot 19) and serum amyloid P component precursor (spot 30), were nitrated in chronic chagasic plasma only. Several other plasma proteins that were nitrated in the acute and/or chronic conditions include α_1-antitrypsin, α_1-fetoprotein (members of the α_1-globulin family), and α- and β- fibrinogen chains.

We also identified six protein spots that matched apolipoprotein A (ApoAI) and were nitrated (two- to threefold) in acute and/or chronic chagasic plasma. The identification of ApoAI in multiple spots can be explained by the fact that ApoAI is expressed as prepro- form (267 amino acids) that is cleaved at N-terminal resulting in formation of a proApoAI (249 amino acids) and mature ApoAI (243 amino acids). Accordingly, of the six ApoAI protein spots, one matched with repeat domain of ApoAI/A4/E and five matched with a precursor or processed form of ApoAI.

Among other nitrated proteins that were detected in the plasma of infected mice, we identified peptides for titin repeat domain of cardiac titin (spots 31 and 32), and the actin repeat domain (spot 33) found in the α-actin and myosin heavy chain. The release of α-actin-, myosin-, and titin peptides was increased by two- to threefold in acute and chronic mice and is indicative of myocyte injury/death. Importantly, 100% of the released α-actin, myosin, and titin peptides were 3NT-modified, suggesting that ROS/RNS-induced myocyte injuries initiated the protein degradation/release.

The proteomic studies also identified the proteins that were changed in expression in acute and chronic chagasic plasma (Tables 1 and 2). The immunoglobulins and immune-related coagulation proteins were, in general, increased in expression level and nitration in both acute and chronic conditions. In contrast, protein level of nitrated ApoAI isoforms was decreased in chronic chagasic plasma (Tables 1 and 2). Other chagasic plasma proteins did not exhibit a change in expression with respect to increase in nitration level. For example, increased nitration of α_1-fetoprotein (spot 2), α_1-antitrypsin (spot 5), and some of the apolipoprotein isoforms (spots

Table 1. Identification of Differentially Expressed/Nitrated Proteins in Chagasic Plasma by MALDI-MS/MS

Spot no.	Protein name	GI no. (NCBI database)	Predicted MW (kd)	Experimental relative MW (kd)	No. of peptide matches
	Albumin family				
1	Albumin precursor	5915682	68	81	9
	α-Globulins				
2	α_1-Fetoprotein	191765	72	77	10
3	α_1-Antitrypsin (α_1-protease inhibitor-2)	191844	53	58	10
4	α_1-Antitrypsin (α_1-protease inhibitor-6)	68068019	53	58	11
5	α_1-Antitrypsin precursor	68068019	53	100	20
	Coagulation proteins				
6	Fibrinogen α chain, C-term globular domain	13529485	55.4	55	24
7	Fibrinogen β chain	15593264	52	52	8
8	Fibrinogen related domain (FReDs)	74143675	50	58	20
	γ-Globulins/Immunoglobulins				
9	Igh-6 protein	31418378	68.5	85	10
10	Igh-6 protein	31418378	68.5	85	6
11	Igh-1a protein	62028521	51.8	52	6
12	IgGγ2a heavy chain	406253	52.2	55	6
13	IgGγ2a heavy chain	406253	52.2	55	7
14	IgGγ3 heavy chain precursor	1304160	52.2	53	4
15	μ (b) haplotype heavy chain	52382	50.7	80	5
16	IgG2b κ light chain, antigen-binding Fab fragment	443113	24	24	7
17	Igκ light chain V-III region	125806	14.5	25	9
18	Igκ light chain, C-region	541736	23.9	24	10
19	Igκ light chain	541736	23.9	27	10
20	IgG1 light chain, nucleic acid-binding Fab fragment	498315	23.3	24	6
21	Agglutinating monoclonal antibody light chain	2950241	24	24	5
22	IgA light chain, Fab fragment to cytochrome P450 aromatase	7766934	24.1	24	7
	Complement				
23	Complement C3 precursor, C3 β chain	1352102	75	55	10
	Apolipoproteins				
24	Apolipoprotein A-I precursor	109571	30.3	27	6
25	Apolipoprotein A-I precursor	109571	30.3	22	7
26	Apolipoprotein A-I precursor	109571	30.3	21	6
27	Apolipoprotein A-I precursor	109571	30.6	22	10
28	Apolipoprotein A-1	61402210	23.0	22	7
29	Apolipoprotein A1/A4/E repeat domain	74149657	30.6	23	12
	Amyloid proteins				
30	Serum amyloid P component precursor	134198	26.1	30	8
	Others				
31	Titin isoform N2-B repeats	77812699	3004	88	69
32	Titin isoform N2-B repeats	77812699	3004	50	67
33	α-Actin 1/spectrin repeats	61218045	45	55	13
34	Unnamed protein	26337783	31.4	50	7
35	Unnamed protein	74140800	101.6	88	5
36	Unnamed protein	74153162	59.4	72	8
37	Unnamed protein	74137565	70.7	90	16
38	Unnamed protein	74203381	70.7	80	21
39	Unnamed protein	26341396	67	76	7

(table continues)

25–29) was not associated with a similar increase in their expression in acute plasma of infected mice. Likewise, many of the proteins (eg, spots 2–4, 36, 43, 44) that were nitrated in chronic conditions were not altered in their expression level in chagasic plasma.

To independently validate the identity of nitrated proteins identified by 2D-GE/WB with anti-3NT antibody and mass spectrometry, we chose to perform WB with protein (ApoAI)-specific antibody. Plasma proteins from normal and acutely infected mice were resolved by 2D-GE and probed with anti-ApoAI antibody or anti-3NT antibody (Figure 8). Anti-ApoAI antibody recognized several protein spots (relative molecular mass range of 23–30 kd) in normal and acute plasma (Figure 8, A and D). Anti-3NT antibody cross-reacted with many of the anti-ApoAI-recognized protein spots in chagasic plasma only (Figure 8, B and

Table 1. Continued

% sequence coverage	Score	Change in expression*		Increase in protein 3-NT formation†	
		Acute	Chronic	Acute	Chronic
33	108	ns	ns	2.8	ns
38	86	ns	ns	3.8	3.6
26	82	1.8	−1.8	3.4	2.2
30	96	2.2	ns	5.1	1.8
51	62	ns	ns	4.7	ns
50	204	4.8	2.3	2.2	1.06
22	79	2.8	1.9	2.3	ns
51	257	2.5	4.3	4.9	2.4
21	108	ns	ns	2.3	ns
22	60	ns	ns	4.2	ns
26	58	4.1	−4.3	5.5	−2.8
28	51	2.5	ns	3.4	1.7
16	55	2.5	ns	6.1	1.2
20	58	3.9	3.3	2.4	1.2
21	58	3.06	2.04	2.8	ns
34	108	3.09	2.65	1.9	ns
41	56	3.7	1.8	1.0	−2.3
20	73	3.9	3.4	1.8	ns
26	46	ns	5.7	ns	1.7
35	84	3.4	3.2	1.7	ns
26	61	3.8	3.2	2.4	1.1
33	70	3.7	3.2	1.5	1.1
27	57	4.2	2.5	3.1	1.5
29	67	3.2	2.6	2.2	1.2
30	69	ns	−2.5	1.8	1.4
20	81	ns	−2.4	1.6	1.4
25	110	ns	−1.8	1.6	1.2
22	87	ns	−2.7	1.1	−1.6
37	122	ns	ns	2.8	1.6
33	77	1.9	2.8	ns	2.5
19	59	3.5	2.2	3.1	ns
15	57	2.6	1.7	2.7	ns
51	71	3.5	2.8	5.5	1.9
35	56	ns	ns	1.6	1.2
21	56	ns	ns	1.5	−3.5
31	56	ns	ns	4.2	2.1
27	93	ns	ns	4.0	1.4
38	186	ns	ns	3.6	ns
25	100	ns	ns	1.4	ns

T. cruzi-infected C3H/HeN mice were sacrificed during acute infection or chronic disease stage. Plasma proteins were resolved by two-dimensional gel electrophoresis, and 3-nitrotyrosine-modified proteins were detected by Western blotting. Differentially nitrated protein spots were sequenced by MALDI-MS/MS. ns, not significant.

*Change in expression is presented as fold change from control; cut-off value was set at ±1.8. Values for repressed genes are log transformed.

†Increase in nitration level is presented as fold change from controls after normalization of background signal. The expression and nitration level was quantitated by densitometric analysis.

E). SYPRO Ruby staining of the gels showed equal loading of all protein samples (Figure 8, C and E). These data verify the identity of nitrated ApoAI in chagasic plasma and validate the identification of proteins by mass spectrometry.

Discussion

We have shown that *T. cruzi* infection-induced oxidative/nitrosative stress affects host proteins. The extent of pro-

Table 2. Additional Differentially Expressed/Nitrated Proteins in Chagasic Plasma Identified by LC-MS/MS Analysis

Spot no.	Protein name	Accession no.	Predicted MW (kd)	Experimental relative MW (kd)	No. of peptide matches	Score	Change in expression*		Increase in protein 3-NT formation†	
							Acute	Chronic	Acute	Chronic
	Albumin family									
40	Serum albumin precursor	IPI0013695	68.6	81	3	100	ns	ns	3.6	ns
41	Serum albumin precursor	IPI0013695	68.6	78	11	128	ns	ns	1.3	ns
42	Serum albumin precursor	IPI0013695	68.6	76	2	108	ns	ns	2.2	ns
	α-Globulins									
43	Trypsinogen 16	IPI00130391	26.1	25	1	40	ns	ns	ns	3.1
44	α-Macroglobulin precursor	IPI00126194	165.7	110	3	20	2.5	ns	ns	2.3
	γ-Globulins/ immunoglobulins									
45	Ig κ chain V-III region MOPC 41 precursor	IPI00137967	14.30	27	1	8	5.7	3.5	1.6	1.6
46	Ig κ chain V-III region MOPC 321 precursor	IPI00464396	14.51	28	2	10	ns	−1.8	ns	ns
47	Ig κ chain V-IV region	IPI00352901	17.1	30	1	10	6.6	9.7	ns	1.7
48	MHC (Qa) Q10-k class 1 antigen	IPI00321666	37.22	28	1	10	5.3	3.1	1.6	1.3
49	Ig κ light chain C region	IPI00406213	23.9	28	1	10	3.8	5.7	2.0	ns
	Others									
50	α-2-HS-glycoprotein precursor		37.3	20	1	10	ns	ns	1.2	ns

T. cruzi-infected C3H/HeN mice were sacrificed during acute or chronic disease stage. Plasma proteins were resolved by two-dimensional gel electrophoresis, and 3-nitrotyrosine modified proteins were detected by Western blotting. Differentially nitrated protein spots were sequenced by LC-MS/MS. ns, not significant.

*Change in expression is presented as fold change from control; cut off value was set at ±1.8. Values for repressed genes are log transformed.

†Increase in nitration level is presented as fold change from controls after normalization of the background signal. The expression and nitration level was quantitated by densitometric analysis.

tein oxidation and nitration in heart tissue and plasma of infected animals correlated with the magnitude of inflammatory responses in acute and chronic conditions. Comparative studies in ethanol-fed animals showed that EICM is slow in development and is and associated with mild inflammatory and oxidative responses in the heart or plasma. We have developed chagasic plasma proteome and identified proteins that are nitrated in disease- and disease state-specific manner.

Our objective in this study was to identify the oxidative/nitrosative modifications that are distinctly enhanced during the course of *T. cruzi* infection and disease development, and may provide clues to pathological process in Chagas' disease. A comparative analysis of cardiac and

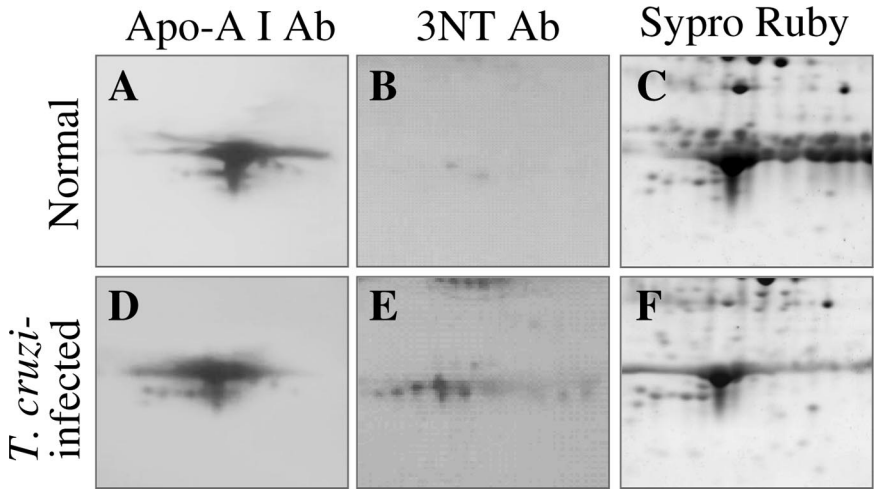

Figure 8. Validation of nitration of apolipoprotein A in chagasic plasma. Dealbuminated plasma fractions from normal **(A–C)** and acutely infected **(D–F)** mice were resolved by 2D-GE and stained with SYPRO Ruby **(C**, **F)**. Proteins were transferred to polyvinylidene difluoride membranes, and Western blot analysis was performed using anti-ApoAI **(A**, **D)** antibody. Membranes were stripped and then probed with anti-3NT **(B**, **E)** antibody.

plasma samples from *T. cruzi*-infected and ethanol-fed animals showed that *T. cruzi*-induced inflammatory responses and oxidative/nitrosative modifications were widely distributed in the heart and plasma of acute animals and persisted during chronic phase. A substantial increase in cardiac protein carbonylation[17] and nitration[21] in animal models of *T. cruzi* infection and disease development has also been shown in previous studies. In ethanol-fed animals, a milder increase in cardiac and plasma level of inflammatory and oxidative responses was noted only after a long-term alcohol feeding. Interestingly, animals with EICM exhibited statistically insignificant change in protein nitration when compared to *T. cruzi*-infected animals that were presented with extensive nitration of plasma and cardiac proteins. The low nitrosative stress and slow evolution of cardiomyopathy in ethanol-fed animals as compared to *T. cruzi*-infected animals suggest that protein nitration plays an important role in Chagas' disease.

During *T. cruzi* infection, macrophage and neutrophil activation play a central role in the antiparasite defense. Several investigators have used *in vitro* assay systems or animal models and demonstrated that *T. cruzi*-mediated macrophage activation result in increased levels of superoxide formation by the NADPH oxidase-dependent respiratory burst.[20,34,35] Besides oxidative stress of inflammatory origin, chagasic host exhibits compromised mitochondrial respiratory chain efficiency in the heart[17,18] that contributes to a substantial increase in ROS generation in cardiomyocytes. Increased expression of XOD (superoxide source), as noted in this study, suggest that endothelial ROS may also be produced in chagasic animals. In addition to ROS, activated macrophages can produce large amounts of NO by iNOS. We have noted plasma NO level, measured by its end product NO_2^-/NO_3^-, increased in response to *T. cruzi* infection and persisted during chronic stage. Others have demonstrated high level of iNOS expression and NO production in splenocytes from *T. cruzi*-infected mice[36] and macrophages *in vitro* infected with *T. cruzi*.[37] Thus, conditions conducive to NO and superoxide reaction resulting in peroxynitrite formation that is a strong nitrating agent exist in *T. cruzi*-infected host. Additionally, enhanced expression of MPO in *T. cruzi*-infected mice, as noted in this study, suggest that MPO-mediated oxidation of nitrite resulting in the formation of highly reactive nitryl chloride would also contribute to protein tyrosine nitration in chagasic host. No change in nitrate/nitrite level in chronic ethanol-fed animals indicates that iNOS-dependent NO production is not induced and explains the absence of nitrosative stress during EICM.

Toward identifying the nitrated proteins that may provide clues to disease-specific pathological processes, we have used a widely accepted 2D proteomic/Western blotting approach to resolve the 3NT-modified plasma proteins in chagasic mice and identified the selected proteins by MALDI-TOF-MS and nanoLC-MS/MS. Our data demonstrate that nitration of plasma proteins was not merely a function of their relative abundance and occurred in a selective manner associated with disease state. A total of 56 protein spots were found to be differentially nitrated in plasma of infected mice during the course of disease development. The sequencing of the nitrated protein spots and clustering of the identified proteins according to their functional characteristics revealed the molecular print of the biological processes that might be perturbed and contribute to parasite persistence and Chagas' disease development.

In vitro studies have shown that ROS/RNS treatment of IgG resulted in decreased antigen-binding capacity and complement C3 and C1q fixation[38] and impaired the Fc receptor binding to macrophages.[39] Oxidation/nitration of IgGs is increased in rheumatoid[40] and juvenile idiopathic arthritis[41] and lupus erythematosus[42] and is implied to be of pathological importance in human autoimmune diseases. In *T. cruzi*-infected animals, several of the light and heavy chains of immunoglobulins and γ-globulins, and the C3b component of the complement system were nitrated (two- to threefold increase) in acute phase, and nitration of a majority of these molecules persisted during chronic stage. Our data provide an impetus to identify the site and extent of nitration in IgG molecules and its effect on antibody assembly and/or activity against the parasite and self-antigens. We propose that if the anti-parasite IgGs are excessively nitrated in the Fab region, it may change the specificity or plasticity of antigen-binding site resulting in decreased recognition of parasite antigens or increased immunoreactivity against self-antigens. Alternatively, if 3NT modifications are accrued in the Fc region, it may alter the binding of the antigen-IgG immune complex to Fc receptor on macrophages, and along with nitrated C3b, result in compromised complement activation/fixation and host's capacity to clear parasite infection. We will pursue identifying the biological impact of IgG nitration on affinity and avidity of anti-parasite antibodies in future studies.

Nitration of two different sets of plasma proteins plays a role in atherosclerotic plaque formation. The nitration of fibrinogen chains (α, β, γ) is suggested to promote a prothrombotic state[43] via its enhanced interaction with thrombin,[44] resulting in accelerated fibrin clot formation that is routinely found in subjects with coronary artery disease.[45] The protective action of ApoAI/high-density lipoprotein in cardiovascular diseases is attributed to its role in reverse cholesterol transport.[46] ApoAI is susceptible to MPO-mediated oxidative chlorination and nitration.[47] Oxidized ApoAI was decreased in its ability to promote adenosine triphosphate-binding cassette A1 (ABCA1)-dependent, low-density lipoprotein-cholesterol efflux from cholesterol-laden macrophages[48] and inhibit inflammatory properties of oxidized low-density lipoproteins.[49] We have noted a two- to fourfold increase in nitration of fibrinogen (α and β chains) and a one- to twofold increase in nitration of ApoAI isoforms in acutely and chronically infected mice (Tables 1 and 2). The nitration of ApoAI isoforms in chagasic plasma occurred in parallel with increased MPO activity (Figure 3). Further, patients with Chagas' disease show the same pattern of atherosclerotic disease as is seen in other cardiomyopathic population after an episode of acute myocardial infarction.[50] Thus, our data along with the observations in literature allow us to propose that persistently nitrated

fibrinogen and ApoAI may result in increased fibrin clot formation and decreased cholesterol efflux, respectively. When present in excess, both these processes can contribute to artery blockage and myocardial infarction, to be further examined in experimental animals and patients with Chagas' disease.

Beyond cholesterol efflux, ApoAI/high-density lipoprotein is shown to regulate cytokine production in monocytes/macrophages via inhibiting the T cell signaling of monocytes, and thereby controls inflammatory cytotoxicity.[51] A decline in ApoAI level is associated with autoimmune inflammatory diseases, eg, juvenile rheumatoid arthritis, systemic lupus erythematosus, and multiple sclerosis,[52] while oxidized ApoAI is suggested to impart proinflammatory properties.[53] Our data show that the ApoAI level was decreased (more than twofold) in chronic mice and more than 50% of the expressed ApoAI was nitrated (Table 1). Chagasic chronic inflammation is characterized by infiltration of inflammatory cells, ie, monocytes and T cells into the heart.[54] Although monocytes/macrophages and stimulated T cells contribute to control of acute parasite infection via release of inflammatory mediators and cytotoxicity against infected cells,[5] the stimuli that contribute to persistence of chronic inflammation in chagasic host are not clearly delineated. We propose that increased 3NT versus normal ApoAI ratio level may result in dysregulated production of cytokines and their respective inhibitors and impart chronic inflammation in Chagas' disease. A significant increase (four- to fivefold, Table 1) in nitration of α_1-antitrypsin, a host defense against toxic enzymes of inflammatory cells,[55] may further exacerbate the inflammation-induced tissue damage in Chagas' disease.

The finding of oxidized peptides representing cytoskeletal proteins (α-actin and titin) in chagasic plasma deserves specific mention. The titin filaments ensure the elasticity and extensibility of the sarcomere and thereby cardiac contractility. Others have shown a loss of titin and reduction of contractile apparatus in heart failure.[56] The myocardial nitrosative stress was increased in acute and chronic animals (Figure 1), and all of the α actin and titin peptides released in the plasma were 3NT-modified (Figures 6 and 7; Table 1). It is thus reasonable to suggest that nitrosative stress-induced cellular injuries initiated protein degradation/release and myocyte damage in chagasic animals. A continuous loss of cytoskeletal proteins due to persistent nitrosative stress in the heart (Figure 1) is anticipated to promote the ventricular stiffness and contribute to heart failure during chronic disease phase and will be examined in future studies.

In summary, we have shown that induction of inflammatory mediators during *T. cruzi* infection elicit oxidative/nitrosative stress that affects host proteins. Many of the plasma proteins were nitrated in a disease-specific manner and would be useful biomarkers of the acute and chronic Chagas' disease states. Further, nitration of specific sets of proteins provided clues to pathophysiology of Chagas' disease. Of significant importance are the observations of increased nitration of immunoglobulins and ApoAI that may provide the basis for parasite persistence/autoimmunity and atherosclerotic responses, respectively, in Chagas' disease.

Acknowledgments

We thank Dr. Z. Gaun for providing plasma and heart tissues from the ethanol-fed rats. We thank the Biomedical Resource Facility and Mass Spectrometry Laboratory at the University of Texas Medical Branch at Galveston, and the Bimolecular Analysis Core Facility at the Border Biomedical Research Center, University of Texas at El Paso, for mass spectrometric analysis. Our thanks are due to Ms. Mardelle Susman for editing the manuscript.

References

1. Higuchi MD, Benvenuti LA, Martins Reis M, Metzger M: Pathophysiology of the heart in Chagas' disease: current status and new developments. Cardiovasc Res 2003, 60:96–107
2. Rossi MA, Ramos SG, Bestetti RB: Chagas' heart disease: clinical-pathological correlation. Front Biosci 2003, 8:e94–e109
3. Leon JS, Engman DM: The significance of autoimmunity in the pathogenesis of Chagas heart disease. Front Biosci 2003, 8:e315–322
4. Tostes S Jr, Bertulucci Rocha-Rodrigues D, de Araujo Pereira G, Rodrigues V Jr: Myocardiocyte apoptosis in heart failure in chronic Chagas' disease. Int J Cardiol 2005, 99:233–237
5. Zacks MA, Wen J-J, Vyatkina G, Bhatia V, Garg N: An overview of chagasic cardiomyopathy: pathogenic importance of oxidative stress. Ann Acad Bras Cienc 2005, 77:695–715
6. Schirmer RH, Schollhammer T, Eisenbrand G, Krauth-Siegel RL: Oxidative stress as a defense mechanism against parasitic infections. Free Radic Res Commun 1987, 3:3–12
7. Cardoni RL, Antunez MI, Morales C, Nantes IR: Release of reactive oxygen species by phagocytic cells in response to live parasites in mice infected with Trypanosoma cruzi. Am J Trop Med Hyg 1997, 56:329–334
8. Cross AR, Yarchover JL, Curnutte JT: The superoxide-generating system of human neutrophils possesses a novel diaphorase activity. Evidence for distinct regulation of electron flow within NADPH oxidase by p67-phox and p47-phox. J Biol Chem 1994, 269:21448–21454
9. Winterbourn CC, Vissers MC, Kettle AJ: Myeloperoxidase. Curr Opin Hematol 2000, 7:53–58
10. Candeias LP, Patel KB, Stratford MR, Wardman P: Free hydroxyl radicals are formed on reaction between the neutrophil-derived species superoxide anion and hypochlorous acid. FEBS Lett 1993, 333:151–153
11. Vespa GN, Cunha FQ, Silva JS: Nitric oxide is involved in control of *Trypanosoma cruzi*-induced parasitemia and directly kills the parasite *in vitro*. Infect Immun 1994, 62:5177–5182
12. Piacenza LPG, Alvarez MN, Kelly JM, Wilkinson SR, Radi R: Peroxiredoxins play a major role in protecting *Trypanosoma cruzi* against macrophage- and endogenously-derived peroxynitrite. Biochem J 2008, 410(2):359–368
13. Beckman JS, Koppenol WH: Nitric oxide, superoxide, and peroxynitrite: the good, the bad, and ugly. Am J Physiol 1996, 271:C1424–1437
14. Wen J-J, Yachelini PC, Sembaj A, Manzur RE, Garg N: Increased oxidative stress is correlated with mitochondrial dysfunction in chagasic patients. Free Radic Biol Med 2006, 41:270–276
15. de Oliveira TB, Pedrosa RC, Filho DW: Oxidative stress in chronic cardiopathy associated with Chagas disease. Int J Cardiol 2007, 116:357–363
16. Perez-Fuentes R, Guegan JF, Barnabe C, Lopez-Colombo A, Salgado-Rosas H, Torres-Rasgado E, Briones B, Romero-Diaz M, Ramos-Jimenez J, Sanchez-Guillen Mdel C: Severity of chronic Chagas disease is associated with cytokine/antioxidant imbalance in chronically infected individuals. Int J Parasitol 2003, 33:293–299
17. Wen J-J, Vyatkina G, Garg N: Oxidative damage during chagasic cardiomyopathy development: role of mitochondrial oxidant release

and inefficient antioxidant defense. Free Radic Biol Med 2004, 37:1821–1833
18. Wen J-J, Bhatia V, Popov VL, Garg NJ: Phenyl-alpha-tert-butyl nitrone reverses mitochondrial decay in acute Chagas disease. Am J Pathol 2006, 169:1953–1964
19. Macao LB, Filho DW, Pedrosa RC, Pereira A, Backes P, Torres MA, Frode TS: Antioxidant therapy attenuates oxidative stress in chronic cardiopathy associated with Chagas' disease, Int J Cardiol 2007, 123:43–49
20. Alvarez MN, Irigoín F, Peluffo G, Radi R: Macrophage-derived peroxynitrite diffusion and toxicity to Trypanosoma cruzi. Arch Biochem Biophys 2004, 432:222–232
21. Naviliat M, Gualco G, Cayota A, Radi R: Protein 3-nitrotyrosine formation during Trypanosoma cruzi infection in mice. Braz J Med Biol Res 2005, 38:1825–1834
22. Lui CY, Guan ZJ, Eskelson CD: Cardiac function in rats exposed to chronic alcohol and nutritional deficiency involving selenium and vitamin E. J Appl Res 2004, 4:427–438
23. Colantonio DA, Dunkinson C, Bovenkamp DE, Van Eyk JE: Effective removal of albumin from serum. Proteomics 2005, 5:3831–3835
24. Buss IH, Winterbourn CC: Protein carbonyl measurement by ELISA. Methods Mol Biol 2002, 186:123–128
25. Sawa T, Akaike T, Maeda H: Tyrosine nitration by peroxynitrite formed from nitric oxide and superoxide generated by xanthine oxidase. J Biol Chem 2000, 275:32467–32474
26. Kleinbongard P, Rassaf T, Dejam A, Kerber S, Kelm M: Griess method for nitrite measurement of aqueous and protein-containing samples. Methods Enzymol 2002, 359:158–168
27. Vodovotz Y: Modified microassay for serum nitrite and nitrate. Biotechniques 1996, 20:390–394
28. Bradley PP, Priebat DA, Christensen RD, Rothstein G: Measurement of cutaneous inflammation: estimation of neutrophil content with an enzyme marker. J Invest Dermatol 1982, 78:206–209
29. Terada LS, Leff JA, Repine JE: Measurement of xanthine oxidase in biological tissues. Methods Enzymol 1990, 186:651–656
30. Buscaglia CA, Campo VA, Di Noia JM, Torrecilhas AC, De Marchi CR, Ferguson MA, Frasch AC, Almeida IC: The surface coat of the mammal-dwelling infective trypomastigote stage of *Trypanosoma cruzi* is formed by highly diverse immunogenic mucins. J Biol Chem 2004, 279:15860–15869
31. Altschul SF, Gish W, Miller W, Myers EW, Lipman DJ: Basic local alignment search tool. J Mol Biol 1990, 215:403–410
32. Doering TL, Lu T, Werbovetz KA, Gokel GW, Hart GW, Gordon JI, Englund PT: Toxicity of myristic acid analogs toward African trypanosomes. Proc Natl Acad Sci USA 1994, 91:9735–9739
33. Miyagi MSH, Darrow RM, Yan L, West KA, Aulak KS, Stuehr DJ, Hollyfield JG, Organisciak DT, Crabb JW: Evidence that light modulates protein nitration in rat retina. Mol Cell Proteomics 2002, 1:293–303
34. Munoz-Fernandez MA, Fernandez MA, Fresno M: Activation of human macrophages for the killing of intracellular Trypanosoma cruzi by TNF-alpha and IFN-gamma through a nitric oxide-dependent mechanism. Immunol Lett 1992, 33:35–40
35. Melo RC, Fabrino DL, D'Avila H, Teixeira HC, Ferreira AP: Production of hydrogen peroxide by peripheral blood monocytes and specific macrophages during experimental infection with Trypanosoma cruzi in vivo. Cell Biol Int 2003, 27:853–861
36. Martins GACM, Aliberti JC, Silva JS: Nitric oxide-induced apoptotic cell death in the acute phase of Trypanosoma cruzi infection in mice. Immunol Lett 1998, 63:113–120
37. Bergeron MOM: Trypanosoma cruzi-mediated IFN-gamma-inducible nitric oxide output in macrophages is regulated by iNOS mRNA stability. J Immunol 2006, 177:6271–6280
38. Uesugi M, Yoshida K, Jasin HE: Inflammatory properties of IgG modified by oxygen radicals and peroxynitrite. J Immunol 2000, 165:6532–6537
39. Margiloff L, Chaplia L, Chow A, Singhal PC, Mattana J: Metal-catalyzed oxidation of immunoglobulin G impairs Fc receptor-mediated binding to macrophages. Free Radic Biol Med 1998, 25:780–785
40. Lemarechal H, Allanore Y, Chenevier-Gobeaux C, Kahan A, Ekindjian OG, Borderie D: Serum protein oxidation in patients with rheumatoid arthritis and effects of infliximab therapy. Clin Chim Acta 2006, 372:147–153
41. Zurawa-Janicka D, Renke J, Popadiuk S, Skorko-Glonek J, Szumera M, Plata-Nazar K, Ulko P, Wozniak M, Lipinska B: Preferential immunoglobulin oxidation in children with juvenile idiopathic arthritis. Scand J Rheumatol 2006, 35:193–200
42. Khan F, Siddiqui AA, Ali R: Measurement and significance of 3-nitrotyrosine in systemic lupus erythematosus. Scand J Immunol 2006, 64:507–514
43. Vadseth C, Souza JM, Thomson L, Seagraves A, Nagaswami C, Scheiner T, Torbet J, Vilaire G, Bennett JS, Murciano JC, Muzykantov V, Penn MS, Hazen SL, Weisel JW, Ischiropoulos H: Pro-thrombotic state induced by post-translational modification of fibrinogen by reactive nitrogen species. J Biol Chem 2004, 279:8820–8826
44. Gole MD, Souza JM, Choi I, Hertkorn C, Malcolm S, Foust RF, 3rd, Finkel B, Lanken PN, Ischiropoulos H: Plasma proteins modified by tyrosine nitration in acute respiratory distress syndrome. Am J Physiol Lung Cell Mol Physiol 2000, 278:L961–L967
45. Parastatidis ITL, Fries DM, Moore RE, Tohyama J, Fu X, Hazen SL, Heijnen HF, Dennehy MK, Liebler DC, Rader DJ, Ischiropoulos Increased protein nitration burden in the atherosclerotic lesions and plasma of apolipoprotein A-I deficient mice, Circ Res 2007, 101:368–376
46. Lewis GF: Determinants of plasma HDL concentrations and reverse cholesterol transport. Curr Opin Cardiol 2006, 21:345–352
47. Nicholls SJ, Zheng L, Hazen SL: Formation of dysfunctional high-density lipoprotein by myeloperoxidase. Trends Cardiovasc Med 2005, 15:212–219
48. Shao B, Bergt C, Fu X, Green P, Voss JC, Oda MN, Oram JF, Heinecke JW: Tyrosine 192 in apolipoprotein A-I is the major site of nitration and chlorination by myeloperoxidase, but only chlorination markedly impairs ABCA1-dependent cholesterol transport. J Biol Chem 2005, 280:5983–5993
49. Navab M, Ananthramaiah GM, Reddy ST, Van Lenten BJ, Ansell BJ, Hama S, Hough G, Bachini E, Grijalva VR, Wagner AC, Shaposhnik Z, Fogelman AM: The double jeopardy of HDL. Ann Med 2005, 37:173–178
50. Marin-Neto JA, Simoes MV, Ayres-Neto EM, Attab-Santos JL, Gallo L Jr, Amorim DS, Maciel BC: Studies of the coronary circulation in Chagas' heart disease. Sao Paulo Med J 1995, 113:826–834
51. Hyka N, Dayer JM, Modoux C, Kohno T, Edwards CK 3rd, Roux-Lombard P, Burger D: Apolipoprotein A-I inhibits the production of interleukin-1beta and tumor necrosis factor-alpha by blocking contact-mediated activation of monocytes by T lymphocytes. Blood 2001, 97:2381–2389
52. Burger D, Dayer JM: High-density lipoprotein-associated apolipoprotein A-I: the missing link between infection and chronic inflammation? Autoimmun Rev 2002, 1:111–117
53. Van Lenten BJ, Hama SY, de Beer FC, Stafforini DM, McIntyre TM, Prescott SM, La Du BN, Fogelman AM, Navab M: Anti-inflammatory HDL becomes pro-inflammatory during the acute phase response: loss of protective effect of HDL against LDL oxidation in aortic wall cell cocultures. J Clin Invest 1995, 96:2758–2767
54. Brener Z, Gazzinelli RT: Immunological control of Trypanosoma cruzi infection and pathogenesis of Chagas' disease. Int Arch Allergy Immunol 1997, 114:103–110
55. Daemen MA, Heemskerk VH, van't Veer C, Denecker G, Wolfs TG, Vandenabeele P, Buurman WA: Functional protection by acute phase proteins alpha(1)-acid glycoprotein and alpha(1)-antitrypsin against ischemia/reperfusion injury by preventing apoptosis and inflammation. Circulation 2000, 102:1420–1426
56. Hein S, Kostin S, Heling A, Maeno Y, Schaper J: The role of the cytoskeleton in heart failure. Cardiovasc Res 2000, 45:273–278